Suppression Effect on Explosive Percolation

Y. S. Cho and B. Kahng

Department of Physics and Astronomy, Seoul National University, Seoul 151-747, Korea
(Received 1 October 2011; published 28 December 2011)

Percolation transitions (PTs) of networks, leading to the formation of a macroscopic cluster, are conventionally considered to be continuous transitions. However, a modified version of the classical random graph model was introduced in which the growth of clusters was suppressed, and a PT occurs explosively at a delayed transition point. Whether the explosive PT is indeed discontinuous or continuous becomes controversial. Here, we show that the behavior of the explosive PT depends on detailed dynamic rules. Thus, when dynamic rules are designed to suppress the growth of all clusters, the discontinuity of the order parameter tends to a finite value as the system size increases, indicating that the explosive PT could be discontinuous.

Percolation transition (PT), i.e., the transition from a disconnected state to a connected one, has been regarded as a fundamental model of phase transitions in nonequilibrium systems [1]. The concept of PT has been extended to the formation of macroscopic clusters in network science. A pioneering model of PT in network science is the classical random graph model introduced by Erdős and Rényi (ER) [2] in which a system composed of a fixed number of vertices N evolves as edges are added. At each evolution step, an edge is added between two vertices, that are randomly selected from among unconnected pairs of vertices. In this model, a quantity, called time, is defined as the number of edges added to the system per node. The ER model has been modified by following the so-called Achlioptas process [3]. The Achlioptas process essentially identifies the dynamics that prevent the creation of a given target pattern by choosing one edge from a given number of randomly selected potential edges. In the modified ER model for the PT, the target pattern is a giant cluster. Thus, an edge to be added to the system should be selected such that the growth of clusters can be systematically suppressed. The principle to take this selection rule is hereafter referred to as the suppression principle (SP).

The dynamic rule originally designed by Achlioptas *et al.* [3] is as follows: in the case of two randomly selected edge candidates, the one actually added to the system is the one minimizing the product or the sum of the sizes of the clusters that are connected by each potential edge. The ER models modified according to the product rule and the sum rule are denoted as ERPR and ERSR models, respectively. In these models, the giant-cluster size increases drastically at the critical point, and therefore, the percolation transition is called explosive percolation. The introduction of an explosive PT model has triggered intensive research on discontinuous PTs in nonequilibrium systems [4–12]. Many models have followed the ERPR and ERSR models, and they display similar transition patterns. Although the explosive PT was regarded as discontinuous in the original

paper [3], recently it has been argued that the transition is continuous in the thermodynamic limit [13–17]. Thus, the issue of whether the explosive PT is indeed discontinuous or continuous remains controversial. In this Letter, we describe the microscopic investigation of the dynamic rules of several explosive percolation models and the surprising finding that these rules do not satisfy the SP. Thus, it is rather natural that the PTs of those models are continuous. However, some other variants of the Achlioptas model satisfying the SP exhibit the pattern of discontinuous PTs within the range of our numerical simulations. Thus, we may state that satisfying the SP is essential for discontinuous PTs in the evolution of complex networks.

To explain the dynamic rule, we classify the types of edge candidate pairs as follows. (i) Both edge candidates e_1 and e_2 are intercluster edges. Clusters of sizes $s_{1a}^{(i)}$ and $s_{1b}^{(i)}$ are connected by the edge e_1, and clusters of sizes $s_{2a}^{(i)}$ and $s_{2b}^{(i)}$ are connected by the edge e_2. In the following discussion, we will use the following notation: $P_1^{(i)} = s_{1a}^{(i)} s_{1b}^{(i)}$, $P_2^{(i)} = s_{2a}^{(i)} s_{2b}^{(i)}$, $S_1^{(i)} = s_{1a}^{(i)} + s_{1b}^{(i)}$, and $S_2^{(i)} = s_{2a}^{(i)} + s_{2b}^{(i)}$. (ii) e_1 is an intracluster edge in a cluster of size $s_1^{(ii)}$, and e_2 is an intercluster edge between two clusters of sizes $s_{2a}^{(ii)}$ and $s_{2b}^{(ii)}$. We denote $P_2^{(ii)} = s_{2a}^{(ii)} s_{2b}^{(ii)}$ and $S_2^{(ii)} = s_{2a}^{(ii)} + s_{2b}^{(ii)}$. (iii) Both e_1 and e_2 are intracluster edges in either the same cluster or two different clusters. These three types of edge candidate pairs are depicted in Fig. 1. On the basis of this classification, we formulated several dynamic rules to determine which edge should be added to the system.

Although the original model [3] seems to follow the basic idea of the Achlioptas process, the dynamic rule has to be more carefully examined. As time approaches the percolation threshold, the mean cluster size increases, and one or both potential edges have a greater possibility of being intracluster as shown in Fig. 2(a). Thus, we have to clarify how to formulate the dynamic rule when intracluster edges are selected as potential edges. Here, we
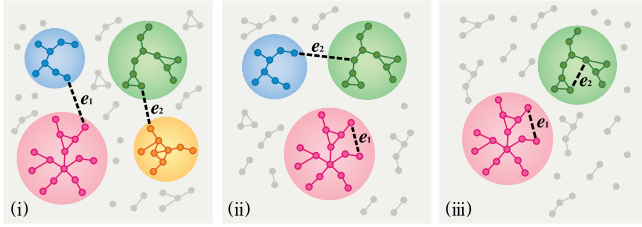
FIG. 1 (color online).   Classification of types of edge candidate pairs. (i) Both candidates e_1 and e_2 are intercluster edges. (ii) e_1 is an intracluster edge and the other candidate e_2 is an intercluster edge. (iii) Both e_1 and e_2 are intracluster edges.

formulate dynamic rules for the cases (i)–(iii), and we check whether each rule does follow the SP.

First, we introduce three different variants of the ERPR model; these are specified in Table I. In model A, when one edge is an intracluster edge [(ii) and (iii)], the product is the square of the size of that cluster, while for case (i), it is the product of the sizes of the two clusters connected by one intercluster edge. This rule, however, can fail to follow the Achlioptas SP. For example, when $s_1^{(ii)} = 5$, $s_{2a}^{(ii)} = 3$, and $s_{2b}^{(ii)} = 7$ for case (ii), the edge e_2 is selected in the ERPR-A model, and then, the size of the created cluster is 10. On the other hand, if edge e_1 is selected, then none of the clusters would increase in size. Therefore, model A does not follow the SP. As the transition point is approached, intracluster edges in (ii) and (iii) can be selected more frequently [see Fig. 2(a)]. Actually, the behavior of the fraction of the occurrences of (ii) or (iii) is similar to that of $G(t)$. Thus the failure of the SP can be more frequent.

In the ERPR-B model, when potential edges of the type (ii) are selected, the intracluster edge is definitely selected, so that the cluster size does not increase. When the two potential edges are both intracluster edges [type (iii)], one of them is randomly selected. By this rule, time is advanced by one unit $1/N$ for the types (ii) and (iii).

Model C is a simplified version of models A and B. In this model, the dynamics proceed via only intercluster connections. Thus, two potential edges are both intercluster edges [case (i)]. Model C may be regarded to be nearly the same as model B because the clusters do not grow when the intracluster edge is selected in (ii) and (iii). However, the difference between them is that for types (ii) and (iii), time is advanced in model B but not in model C.

For all models A, B, and C, the product rule has an intrinsic drawback that the Achlioptas SP is unfulfilled. Let us consider a simple example of two intercluster connections, in which $s_{1a}^{(i)} = 2$, $s_{1b}^{(i)} = 7$, $s_{2a}^{(i)} = 4$, and $s_{2b}^{(i)} = 4$. Then, $P_1^{(i)} = 14$ and $P_2^{(i)} = 16$, and thus, edge e_1 is added to the system. However, the resulting cluster size is 9 in the case, which is larger than the resulting size 8 when e_2 is added. In other words, even though the product of one pair of cluster sizes is smaller than that of the other pair, its sum can be larger. Thus, the Achlioptas SP is inherently
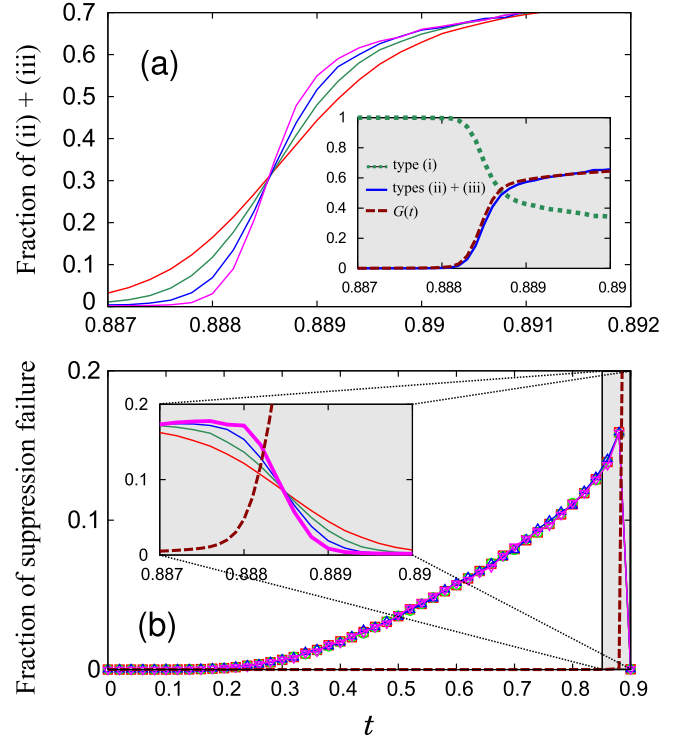

FIG. 2 (color online).   (a) The fractions of type (ii) and type (iii) potential edges as a function of time t for different system sizes: $N/10^4 = 32, 64, 128,$ and 256 from the top (bottom) in the small-t (large-t) region. As N increases, the fraction increases dramatically. Inset: For a given $N = 1.024 \times 10^7$, the fractions of the type (i) (dotted line) and the types (ii) and (iii) (solid lines) as a function of t. They are compared with the giant-cluster size $G_N(t)$ (dashed line). The fraction of the types (ii) or (iii) behaves similarly to $G_N(t)$, indicating that counting for the effect by taking the intracluster edges becomes important as t approaches t_c. (b) The fraction of the occurrences in which the sum of the sizes of one pair of clusters becomes larger than that of the size of the other pair, even though the product of the sizes of the former is smaller than that of the sizes of the latter. The dotted line represents $G_N(t)$. Inset: Solid lines represent the failure ratio on an enlarged scale for different system sizes $N/10^4 = 32, 64, 128,$ and 256. For a larger system, the curve lies on the upper position in the small-t region. The dashed line represents $G_N(t)$. Numerical data for (a) and (b) are obtained from the ERPR-B model.

unfulfilled. Investigations [5,10,13,16] have shown that the cluster size distribution displays a hump shape in the region of large cluster sizes, and the hump size increases up to the point where explosive cluster aggregations start. Owing to the inherent drawback, such a case is likely to occur frequently, as shown in Fig. 2(b). Thus, the PTs under the product rule are continuous regardless of the model type.

Next, we introduce similar models under the sum rule; these are also listed in Table I. The drawback inherent to the product rule is removed in the ERSR model. However, for case (ii), the Achlioptas SP cannot be fulfilled in

TABLE I.   List of the dynamic rules under the product rule (the sum rule). The second column lists the type of potential edges. The third and fourth columns list the conditions for the cases in which both e_1 and e_2 in Fig. 1 are selected. The last column shows the case when either e_1 or e_2 is selected randomly.

Model	Type	e_1	e_2	Either e_1 or e_2 randomly
Model A	Type (i)	$P_1^{(i)} < P_2^{(i)} \ [S_1^{(i)} < S_2^{(i)}]$	$P_1^{(i)} > P_2^{(i)} \ [S_1^{(i)} > S_2^{(i)}]$	$P_1^{(i)} = P_2^{(i)} \ [S_1^{(i)} = S_2^{(i)}]$
	Type (ii)	$(s_1^{(ii)})^2 < P_2^{(ii)} \ [2s_1^{(ii)} < S_2^{(ii)}]$	$(s_1^{(ii)})^2 > P_2^{(ii)} \ [2s_1^{(ii)} > S_2^{(ii)}]$	$(s_1^{(ii)})^2 = P_2^{(ii)} \ [2s_1^{(ii)} = S_2^{(ii)}]$
	Type (iii)			Unconditional
Model B	Type (i)	$P_1^{(i)} < P_2^{(i)} \ [S_1^{(i)} < S_2^{(i)}]$	$P_1^{(i)} > P_2^{(i)} \ [S_1^{(i)} > S_2^{(i)}]$	$P_1^{(i)} = P_2^{(i)} \ [S_1^{(i)} = S_2^{(i)}]$
	Type (ii)	Unconditional		
	Type (iii)			Unconditional
Model C	Type (i)	$P_1^{(i)} < P_2^{(i)} \ [S_1^{(i)} < S_2^{(i)}]$	$P_1^{(i)} > P_2^{(i)} \ [S_1^{(i)} > S_2^{(i)}]$	$P_1^{(i)} = P_2^{(i)} \ [S_1^{(i)} = S_2^{(i)}]$

model A, but it is always fulfilled in models B and C. Thus, in the case of the sum rule, the models B and C are regarded to be the ones following the Achlioptas SP. We state that the PTs for models B and C are possible candidates for the discontinuous PT.

Even though it is a challenging task to determine the transition types of the explosive PTs with numerical simulation data, the numerical approach is the only one possible, since there is no analytic solution that takes into account all the aforementioned cases. Extensive numerical simulations are carried out up to a system size $N = 10^{10}$ with a configuration average of about $10^{13}/N$. The obtained numerical data may be sufficient for understanding why this controversy has arisen, but a higher configuration average may be required for determining the type of PT, particularly when the system size is large.

We measure $G_N(t)$ as a function of time t for different system sizes in the range $N = 2^0 \times 10^4 - 2^{20} \times 10^4$ at every $N = 2 \times 10^4$ step. For given N and $2N$, we find a point of intersection of the two curves $G_N(t)$ and $G_{2N}(t)$. The time and G components of such a point are denoted as $t_x(2N)$ and $G_{2N}(t_x(2N))$, respectively. We compose a set of $\{t_x(N), G_N(t_x(N))\}$ for the simulated system sizes. To evaluate the discontinuity of the PT, we propose the following criteria: (a) The value $(t_x(N), G_N(t_x))$ remains finite as $N \to \infty$. The time $t_x(\infty)$ is regarded as the transition point t_c in the thermodynamic limit. (b) The tangent of the curve $G_N(t)$ with respect to t at $t_x(N)$ diverges as N increases.

Figures 3(a)–3(c) show the behaviors of $G_N(t_x)$ as a function of N for models A, B, and C, respectively, under the product rule. The insets of each figure show $G_N(t)$ versus t. We can see in (a) and (c) that for the model A and C under the product rule, $G_N(t_x)$ decreases with increasing N in the whole considered range, suggesting that $G_N(t_c) \to 0$ in the limit $N \to \infty$. In the case of model B, even though the data look flat up to $N \simeq 10^8$, they decay in the large-N region in the same manner as for model C. Thus, the decay behavior can be considered to stem from the intrinsic drawback of the product rule for the case (i). In our previous study [10], we performed numerical simulations for the model B under the product rule up to a system

size $N = 10^8$. In that case, however, the decay behavior was not noticed and the PT was regarded as a discontinuous transition. With the simulation data obtained in this study for larger system sizes, we conclude that the three models based on the product rule show continuous PTs.

Figures 3(d)–3(f) are the plots of $G_N(t_x)$ versus N for models A, B, and C under the sum rule. It can easily be seen that for model A, the $G_N(t_x)$ values decrease with increasing N, suggesting that $G_N(t_c)$ is zero in the limit $N \to \infty$. This indicates that the rule of doubling the cluster size in the ERSR-A model violates the SP, and leads to a continuous transition. However, for models B and C, the data of the $G_N(t_x)$ values look relatively flat asymptotically within the large-N limit, even though the data points beyond $N = 10^9$ have large error bars owing to a smaller number of configuration averages. Figure 3(g) shows the tangent to the curve $G_N(t)$ at the crossing point as a function of N. The data show that the tangent increases according to a power law $\sim N^{0.5}$. Thus, we may conclude that the ERSR-B and ERSR-C models fulfill the SP and seem to show discontinuous PTs, within the range of our numerical data. However, we cannot rule out the possibility that the value of $G_N(t_x(N))$ decreases when the system sizes are larger than those simulated in this work.

Recently, the authors [13] introduced a new type of Achlioptas percolation model and argued that the explosive PT is actually continuous. This model, called the CDGM model following the initials of the authors, is defined as follows. First, a pair of clusters, C_{1a} and C_{1b}, are randomly selected and the smaller cluster (say C_{1a}) is selected. Second, another pair of clusters C_{2a} and C_{2b} are randomly picked, and the smaller one (say C_{2a}) is selected. Third, two random nodes from each of the chosen clusters (C_{1a} and C_{2a}) are selected and connected. There are four possible combinations of the connection. However, when either of the two clusters from the first set is identical to either of the two clusters from the second set [for example, C_{1b} and C_{2b} in Fig. 4(a)], the CDGM model can fail to follow the Achlioptas SP. According to the original rule of the CDGM model, the two smaller clusters C_{1a} and C_{2a} are connected, which creates a larger cluster size, whereas the connection between two nodes inside the cluster
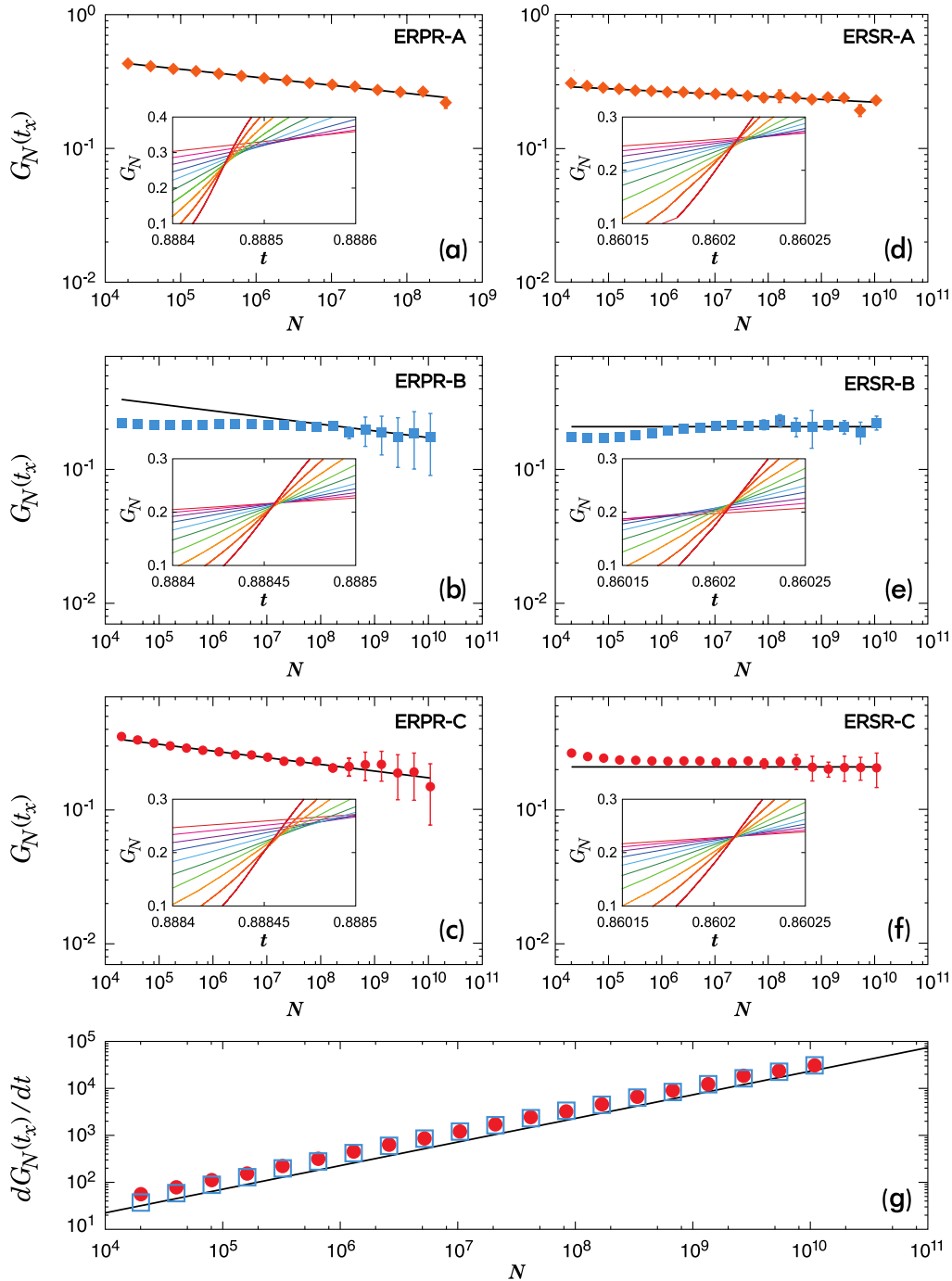
FIG. 3 (color online). $G_N(t_x)$ versus N for the (a) ERPR-A, (b) ERPR-B, (c) ERPR-C, (d) ERSR-A, (e) ERSR-B, and (f) ERSR-C models. The slopes of each guideline is (a) -0.06, (b) -0.05, (c) -0.05, (d) -0.02, (e) 0, and (f) 0. Thus, $G_N(t_x)$ of ERSR-B and ERSR-C converge to finite values in the thermodynamic limit. The error bars represent the deviation of the cross points. Each data set is obtained by taking an average over about $10^{13}/N$ configurations. $G_N(t_x)$ of models B and C of both the ERPR and ERSR overlap in the large-N region. The insets of (a)–(f) show the behaviors of $G_N(t)$ for different system sizes $N/10^4 = 32, 64, 128, 256, 512, 1024,$ 2048, 4096, 8192, and 16384. (g) Plot of the slope of $G_N(t)$ at t_x versus N for the ERSR-B ($\square$) and the ERSR-C ($\bigcirc$) models. $dG_N(t_x)/dt$ increases according to a power law $\sim N^{0.5}$.

$C_{1b} = C_{2b}$ does not increase any cluster size in the system. Therefore, the original CDGM model fails to follow the Achlioptas SP by not taking into account the natural choice of that intracluster edge. Again, as time approaches t_c, the

selection of an intracluster edge becomes more frequent. Thus, the selection of intercluster edges, which is against the SP, can change the PT into a continuous transition. We confirm this result by performing the following numerical
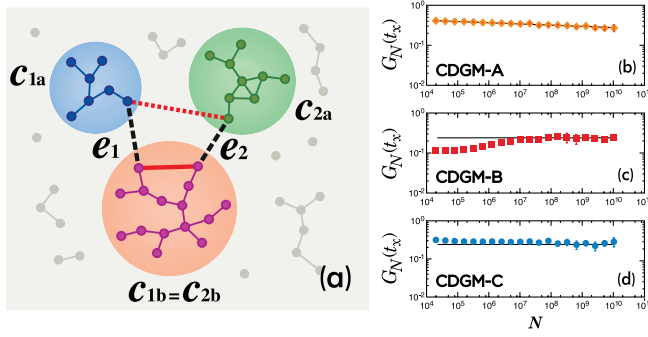
FIG. 4 (color online). (a) Schematic illustration of the selection rule on the intracluster edge for the CDGM-B model. In the original CDGM model (CDGM-A), when two pairs of edges e_1 and e_2 are selected from the cluster sets C_1 and C_2 of sizes $s_{1a} < s_{1b}$ and $s_{2a} < s_{2b}$, an additional edge connects the two nodes in the clusters C_{1a} and C_{2a} (dotted line). In our modified model (CDMA-B) the two nodes in the clusters C_{1b} and C_{2b} are connected instead (solid line), because by choosing them, the cluster sizes in the system do not increase. Panels (b)–(d) show $G_N(t_x)$ versus N for CDGM-A, CDGM-B, and CDGM-C models, respectively, and the slopes are -0.03, 0, and 0, respectively. $G_N(t_x)$ of the models B and C overlap in the large N region. It may be reasonable to expect that the modified CDGM model (CDGM-B and C) shows a discontinuous PT.

simulations. We plot $G_N(t_x)$ versus N, and find $G_N(t_x) \sim N^{-0.03}$ for the CDGM model [Fig. 4(b)]. We then modify the original model as follows: when one or two intracluster edges are present among the four edge candidates, one of these intracluster candidates is connected (model B) randomly. In addition, we consider a model C in which the four edge candidates are only allowed to be intercluster edges. Figures 4(c) and 4(d) suggest that $G_N(t_x)$ approaches a constant value in the large-N region for models B and C, respectively. Moreover, we confirm that the slope of $G_N(t)$ at t_x diverges as N increases in a power law manner. Based on these numerical results, it reveals that the PT could be discontinuous even in the CDGM model, when properly modified.

In summary, we have examined the dynamic rule of the Achlioptas model in the perspective of the suppression principle (SP). We found that when the dynamic rule does follow the SP, the numerically calculated order parameter seems to show the behavior of a discontinuous transition. Otherwise, the PT seems to be continuous. The original Achlioptas model and the CDGM model belong to the latter case. An analytic study of the modified Achlioptas models by taking into account the suppression effect is therefore needed.

[1] D. Stauffer and A. Aharony, *Introduction to Percolation Theory* (Taylor & Francis, London, 1994).
[2] P. Erdős and A. Rényi, Publ. Math. Inst. Hung. Acad. Sci. **5**, 17 (1960).
[3] D. Achlioptas, R. M. D'Souza, and J. Spencer, Science **323**, 1453 (2009).
[4] R. M. Ziff, Phys. Rev. Lett. **103**, 045701 (2009).
[5] Y. S. Cho, J. S. Kim, J. Park, B. Kahng, and D. Kim, Phys. Rev. Lett. **103**, 135702 (2009).
[6] F. Radicchi and S. Fortunato, Phys. Rev. Lett. **103**, 168701 (2009).
[7] E. J. Friedman and A. S. Landsberg, Phys. Rev. Lett. **103**, 255701 (2009).
[8] A. A Moreira, E. A. Oliveira, S. D. S. Reis, H. J. Herrmann, and J. S. Andrade Jr., Phys. Rev. E **81**, 040101 (2010).
[9] Y. S. Cho, B. Kahng, and D. Kim, Phys. Rev. E **81**, 030103 (2010).
[10] Y. S. Cho, S.-W. Kim, J. D. Noh, B. Kahng, and D. Kim, Phys. Rev. E **82**, 042102 (2010).
[11] R. M. D'Souza and M. Mitzenmacher, Phys. Rev. Lett. **104**, 195702 (2010).
[12] N. A. M. Araújo and H. J. Herrmann, Phys. Rev. Lett. **105**, 035701 (2010).
[13] R. A. da Costa, S. N. Dorogovtsev, A. V. Goltsev, and J. F. F. Mendes, Phys. Rev. Lett. **105**, 255701 (2010).
[14] P. Grassberger, C. Christensen, G. Bizhani, S.-W. Son, and M. Paczuski, Phys. Rev. Lett. **106**, 225701 (2011).
[15] J. S. Andrade Jr., H. J. Herrmann, A. A. Moreira, and C. L. N. Oliveira, Phys. Rev. E **83**, 031133 (2011).
[16] H. K. Lee, B. J. Kim, and H. Park, Phys. Rev. E **84**, 020101 (R) (2011).
[17] O. Riordan and L. Warnke, Science **333**, 322 (2011).